in the zone of reduced shear stress downstream of the undular hydraulic jump. Grains below this cutoff size can be transported in suspension across the front and through the jump. They are then available for deposition farther downstream, giving rise to the sand tail (Fig. 1).

Our results show that significant downstream fining can be produced over short distances in the laboratory through selective deposition. We cannot specify precisely the critical factors required to produce well-developed fining but, in our view, the most important respects in which our experiment differed from previous ones were the wide size range and bimodality of the feed mixture and the channel length. In a similar series of detailed experiments performed in a smaller channel, Wilcock and McArdell (*28*) showed that there were strong deviations from equal mobility using the sediment mixture we used in our experiment; fractional transport rates vary inversely with grain size, and the critical shear stress to initiate motion of individual sizes increases with grain size over an order of magnitude. It is likely that both the bimodality of the grain-size distribution and its large standard deviation are important in producing the size-dependent variation in mobility (*29*).

Our results also indicate some factors that are apparently not required to produce strong downstream fining; neither variation in discharge (temporal or spatial) nor preexisting slope variations were present in our experiment. For the simple experimental geometry reported here, downstream fining by selective deposition appears to require only the transport and deposition of a sufficiently poorly sorted or bimodal gravel.

REFERENCES AND NOTES

1. R. D. Russell, in *Recent Marine Sediments*, P. D. Trask, Ed. (Spec. Publ. 4, Society of Economic Paleontologists and Mineralogists, Tulsa, OK, 1955).
2. K. M. Scott and G. C. Gravlee, *U.S. Geol. Surv. Prof. Pap. 422M* (1968).
3. W. C. Bradley, R. K. Fahnestock, E. T. Rowekamp, *Geol. Soc. Am. Bull.* **83**, 1261 (1972).
4. M. Church, *Geol. Surv. Can. Bull. 216* (1972).
5. W. C. Krumbein, *J. Geol.* **49**, 482 (1941).
6. W. J. Plumley, *ibid.* **56**, 526 (1948).
7. P. H. Kuenen, *ibid.* **64**, 336 (1956).
8. P. L. Abbott and G. L. Peterson, *J. Sediment. Petrol.* **48**, 31 (1978).
9. J. Adams, *Science* **203**, 171 (1979).
10. J. Shaw and R. Kellerhals, *The Composition of Recent Alluvial Gravels in Alberta River Beds* (*Bull. 41*, Alberta Research Council, Calgary, 1982).
11. H. Sternberg, *Z. Bauwes.* **25**, 483 (1875).
12. W. C. Bradley, *Geol. Soc. Am. Bull.* **81**, 61 (1970).
13. A. J. Moss, P. H. Walker, J. Hutka, *Sedimentology* **20**, 489 (1973).
14. Y. Kodama, *Environmental Research Paper 15* (Tsukuba Univ., Tsukuba, Japan, 1992).
15. G. Parker, P. C. Klingeman, D. L. McLean, *J. Hydraul. Eng.* **108**, 544 (1982).
16. G. Parker, S. Dhamotharan, H. Stefan, *Water Resour. Res.* **18**, 1395 (1982).
17. E. D. Andrews and D. C. Erman, *ibid.* **22**, 191 (1986).
18. P. L. Wiberg and J. D. Smith, *ibid.* **23**, 471 (1987).
19. P. D. Komar, *J. Sediment. Petrol.* **57**, 203 (1987).
20. P. R. Wilcock and J. B. Southard, *Water Resour. Res.* **24**, 1137 (1988).
21. P. J. Ashworth and R. I. Ferguson, *ibid.* **25**, 627 (1989).
22. P. D. Komar, *Eos* **70**, 320 (1989).
23. P. R. Wilcock and J. B. Southard, *Water Resour. Res.* **25**, 1629 (1989).
24. M. Church *et al.*, *ibid.* **27**, 2941 (1991).
25. L. G. Straub, *Trans. Am. Geophys. Union* **16**, 463 (1935).
26. Y. Kodama, H. Ikeda, H. Iijima, *Bull. 16* (Tsukuba University Center for Hydraulic Experimentation, Tsukuba, Japan, 1992), pp. 119–123.
27. R. Ferguson and P. Ashworth, *Earth Surf. Processes Landforms* **16**, 65 (1991).
28. P. R. Wilcock and B. W. McArdell, *Water Resour. Res.*, in press.
29. P. R. Wilcock, in *Dynamics of Gravel-Bed Rivers*, P. Billi, R. D. Hey, C. R. Thorne, P. Tacconi, Eds. (Wiley, Chichester, 1992), pp. 109–139.

30. We thank H. Ikeda for sharing the results of his experiments on grain sorting. Supported by NSF grants EAR 9004206 and EAR 9004756.

21 July 1992; accepted 2 November 1992

Synchronism of the Siberian Traps and the Permian-Triassic Boundary

I. H. Campbell, G. K. Czamanske, V. A. Fedorenko, R. I. Hill,* V. Stepanov

Uranium-lead ages from an ion probe were taken for zircons from the ore-bearing Noril'sk I intrusion that is comagmatic with, and intrusive to, the Siberian Traps. These values match, within an experimental error of ±4 million years, the dates for zircons extracted from a tuff at the Permian-Triassic (P-Tr) boundary. The results are consistent with the hypothesis that the P-Tr extinction was caused by the Siberian basaltic flood volcanism. It is likely that the eruption of these magmas was accompanied by the injection of large amounts of sulfur dioxide into the upper atmosphere, which may have led to global cooling and to expansion of the polar ice cap. The P-Tr extinction event may have been caused by a combination of acid rain and global cooling as well as rapid and extreme changes in sea level resulting from expansion of the polar ice cap.

It has recently been suggested that flood volcanism is produced by melting of the head of starting plumes that originate at the core-mantle boundary and grow by entrainment as they rise. Thus, by the time they reach the top of the mantle they form giant disks with a diameter of ~2000 km (*1*). This hypothesis offers a simple explanation for the vast lateral extent (typically 2000 by 2000 km) and short duration (1 to 2 million years) of flood volcanism (*2*). Flood volcanic provinces represent the most dramatic outpourings of basalt in the Phanerozoic record, with eruptive rates that are one to two orders of magnitude greater than those associated with normal oceanic hotspots (*3*).

At least ten mass extinctions have been recognized during the last 250 million years. Nine of these, including the two largest at the Cretaceous-Tertiary (K-T) and P-Tr boundaries, may be temporally associated with episodes of flood volcanism (*4*). Recent data for the P-Tr boundary and Siberian Traps, in particular, permit a correlation between the two events. The age of the P-Tr boundary is 251.1 ± 3.6 million years (2σ) based on ion probe analysis (*5*) of zircons extracted from a bentonite layer from the Meishan section at Changing, China. This value agrees with an earlier averaged estimate of 249 ± 4 million years from K-Ar data (*4*). Renne and Basu (*6*) reported whole-rock and plagioclase ^{40}Ar-^{39}Ar incremental heating data for flows from the Siberian flood basalts that indicate that flood basalt volcanism commenced at 248.4 ± 2.4 million years (2σ). Dalrymple *et al.* (*7*) obtained ages of 243.5 ± 1.8 and 244.9 ± 1.8 million years by ^{40}Ar-^{39}Ar laser incremental heating of plagioclase separates from apparently fresh flood basalt drill core from within 300 m of the base of the basalt sequence. These results were duplicated by Baksi and Farrar (*8*) who obtained similar ages of 243 to 244 ± 1.2 million years by whole-rock ^{40}Ar-^{39}Ar laser incremental heating of a sample from the lowest flows of the same drill hole. The discrepancy between these results and those of Renne and Basu arises largely from differences in the age ascribed to the neutron flux monitor MMhb-1 by the different laboratories: Renne and Basu used 520.4 ± 1.7 million years, whereas Dalrymple and colleagues and Baksi and Farrar used 513.9 ± 2.3 million years (*9*). If this

I. H. Campbell and R. I. Hill, Research School of Earth Sciences, Australian National University, Canberra, Australia.
G. K. Czamanske, U.S. Geological Survey, 345 Middlefield Road, Menlo Park, CA 94025.
V. E. Fedorenko and V. Stepanov, Central Research Institute of Geological Prospecting for Base and Precious Metals, Varshavskoye, Shosse 129B, Moscow 113545, Russia.

*Deceased.

Table 1. Earlier Ar-Ar ages for the Siberian Traps, calculated for different ages of the MMhb-1 Standard. Except in Fig. 1, all errors quoted in this paper are two standard deviations.

Study	Rock type	Material	Age (million years)	
			MMhb-1 = 513.9	MMhb-1 = 520.4
Dalrymple *et al.* (*7*)	Ore vein	Biotite	249.0 ± 1.6	252.2 ± 1.6
Renne and Basu (*6*)	Basalt	Whole rock	245.3 ± 2.4	248.4 ± 2.4
Baksi and Farrar (*8*)	Basalt	Plagioclase	243 to 244	246 to 247
Dalrymple *et al.* (*7*)	Basalt	Plagioclase	243.5 ± 1.8	246.6 ± 1.8
Dalrymple *et al.* (*7*)	Basalt	Plagioclase	244.9 ± 1.8	248.0 ± 1.8

difference is considered, there is no statistical difference between the ages obtained by the various laboratories for the age of Siberian Trap volcanism (Table 1).

Age spectra from ^{40}Ar-^{39}Ar dating for biotite from the Noril'sk I intrusion, which intrudes the lower basalt suites, are inconsistent with these data (*7*). Two biotite separates from this intrusion gave disturbed spectra, whereas a third biotite from an ore-bearing vein in the Zapolyarny mine gave a reproducible plateau at 249.0 ± 1.6 million years (2σ), 4 million years older than ages obtained for basalts from the lower part of the sequence. Dalrymple *et al.* (*7*) suggested that the low ages measured for the basalts reflect ^{40}Ar loss from even the freshest materials, despite apparent plateaus in their plagioclase spectra. Alternatively, the third biotite may contain a small amount of excess argon, although there is no evidence in the age spectra to suggest so.

We avoided problems associated with differences in techniques by dating the Siberian Traps and P-Tr boundary in the same laboratory against the same standard. We dated zircons from the Noril'sk I intrusion, which is considered comagmatic with the Siberian Traps, by the SHRIMP ion microprobe following the procedure used by Claoué-Long *et al.* (*5*).

The dated sample is a pegmatoidal taxitic gabbrodolerite from the Medvezhy Creek open pit mine in the Noril'sk I intrusion. This intrusion cuts the two lowest basalt suites (~300 m thick) of the 3500-m-thick section of flood basalt in the Noril'sk area and is similar to other ore-bearing intrusions, emplaced as high as 500 m above the base of the traps. Wooden *et al.* (*10*) have shown that these intrusions have the distinctive chemical and isotopic characteristics of the Siberian Traps and that they best correlate with the basalts of the Morongovsky suite, the seventh of the 11 suites that make up the basalt sequence in the Noril'sk area (*11*). Thus, the Noril'sk I intrusion is associated with the start of the voluminous third cycle of volcanism that produced the upper two-thirds of the basalt sequence in the Noril'sk area and an even greater proportion of the sequence elsewhere. Our data also give the age of the Ni-Cu–platinum group element mineralization at Noril'sk.

Several hundred zircon crystals were extracted from a 1.9-kg sample. Most were clear prisms that show fine growth zoning; a number of grains contained centrally located glass inclusions. Analytical methods followed those in (*5*) except that a power law rather than a polynomial fit was used in comparison of the standard and sample zircon data (*12*). The data were collected on four separate days (Table 2). Most analyzed areas were rich in U and Th, containing 100 to 3800 ppm of U (median 1200 ppm) and 100 to 7100 ppm of Th (median 2600 ppm). The $^{206}Pb/^{238}U$ ages were calculated on the assumption that all analyses are concordant (*13*) and that the excess common lead in some samples has the composition measured for sulfides from the Noril'sk I intrusion (*10*). Six analyses that fall well outside the remainder of the data were excluded from the calculations (Fig. 1). A weighted mean age, calculated by both the power law and polynomial methods, is reported for each day. For the polynomial fit, the mean of days 1 and 2, measured at a high uranium oxide to uranium (UO/U) ratio, is 9 million years greater than for days 3 and 4, measured at a lower UO/U ratio. However, if the preferred power-law fit is used, the difference is well within experimental error. This difference illustrates the improved fit to the data from

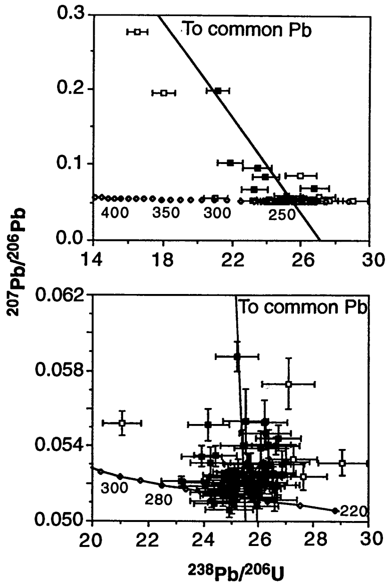

Fig. 1. Tera-Wasserburg–type concordia diagrams showing measured data for Noril'sk zircons. The lower plot is a much enlarged version showing that the majority of the data lie close to concordia at an age of 248.0 ± 3.7 million years. Diamonds show position of concordia; numbers give ages in millions of years. Errors shown are one standard deviation. Common lead has coordinates $^{207}Pb/^{206}Pb$ = 0.8592, $^{238}U/^{206}Pb$ = 0.

Table 2. Summary of SHRIMP data for Noril'sk zircons. The UO/U ratios are for the unknown. Ion probe errors are quoted as SEM at the 95% confidence level. For high UO/U values the polynomial fit gives a higher age than the power law fit, whereas for low UO/U values the reverse is true. At intermediate values, such as those in (*5, 12*), the difference is small. Numbers in parentheses indicate the last significant digits of the $^{206}Pb/^{238}U$ ratio.

Session	Median standards	UO/U	Number	Polynomial fit			Power-law fit		
				$^{206}Pb/^{238}U$ ± $1\sigma_{mean}$	Age (million years) ± $2\sigma_{mean}$	Number deleted	$^{206}Pb/^{238}U$ ± $1\sigma_{mean}$	Age (million years) ± $2\sigma_{mean}$	Number deleted
Day 1	8.0	9.4	24	0.04041 (45)	255.4 ± 5.5	2	0.03980 (41)	251.6 ± 5.0	2
Day 2	8.8	9.6	20	0.03949 (44)	249.6 ± 5.5	2	0.03885 (43)	245.7 ± 5.3	2
Day 3	5.4	6.1	18	0.03824 (43)	241.9 ± 5.2	0	0.03855 (39)	243.8 ± 4.9	0
Day 4	5.3	5.9	21	0.03875 (41)	245.1 ± 5.5	2	0.03967 (38)	250.8 ± 4.8	4
Mean			83	0.03919 (47)	247.8 ± 6.0	6	0.03922 (31)	248.0 ± 3.7	8
P-Tr boundary zircons (*5, 12*)									
Day 1	7.5	7.8	37	0.03973	251.2 ± 3.4 (*5*)	3		251.1 ± 3.6 (*12*)	3
Day 2	6.8	7.2		± 0.00028					

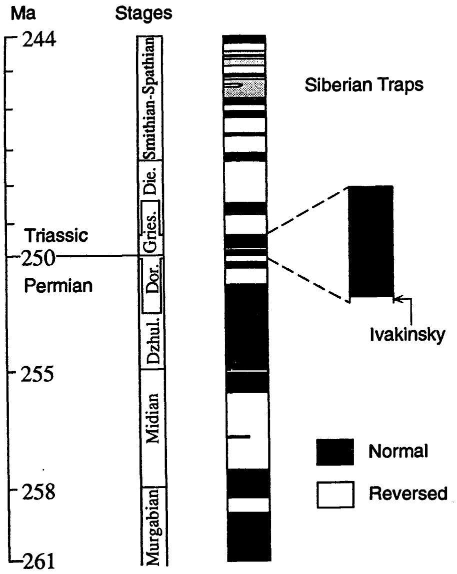

Fig. 2. Composite magnetostratigraphic polarity profile for the P-Tr boundary and the Siberian Traps. Note that time scales are not linear and that they differ for the P-Tr boundary and Siberian Traps. Modified from (*16*). Abbreviations: Dzhul., Dzhulfian; Dor., Dorashamian; Gries., Griesbachian; and Die., Dienerian.

the power law (*12*). The weighted mean age for the four analytical sessions is 248 ± 4 million years, which is not statistically different from the ion probe age of 251 ± 4 million years for the P-Tr boundary.

The Siberian flood basalt province is now thought to extend beneath younger cover to the Ural Mountains and the Taimyr Peninsula (*14*). This estimate almost doubles its known extent (to an area of over 2.5×10^6 km^2 and a volume of at least 2×10^6 to 3×10^6 km^3) and makes it the largest subaerial volcanic event in the Phanerozoic record. Thus, the Siberian Traps and Deccan Traps, two of the largest subaerial volcanic events in the Phanerozoic, appear to correlate with the two most significant extinction events. Much larger submarine volcanic events, such as the one that produced the Ontong-Java plateau (*3*), do not appear to be temporally associated with a global mass extinction.

Furthermore, eruption of the Siberian Traps appears to have been rapid. Comprehensive paleomagmatic studies show that, with the exception of the earliest Ivakinsky suite, the traps and the ore-bearing intrusions erupted during a single period of normal polarity. Magnetostratigraphic studies show that the Earth's magnetic field had a constant reversed polarity for about 60 million years between the Upper Carboniferous and the Upper Permian. This period was followed first by a time in the Late Permian when reversals averaged about 1 million years and then by the Illawarra reversals, a period of rapid reversals in the Lower Triassic. If the eruption of the traps coincides with the P-Tr boundary, the Ivakinsky suite correlates with the period of reversed polarity at the end of the Permian and the remainder of the traps were formed in the period of normal polarity at the base of the Triassic (*15, 16*). From this correlation, the Siberian Traps were erupted during an interval of ~600,000 years or less (Fig. 2). If the traps are younger than the P-Tr boundary, the eruption time may have been even shorter. Age and stratigraphic constraints preclude the possibility that the traps are entirely Permian (*17*).

The P-Tr extinction event, described by Raup and Sepkoski (*18*) as the most important in the Phanerozoic record, is best seen in shallow water benthic fauna. It is associated with a period of rapid sea-level fluctuations with an estimated maximum fall in sea level of up to 280 m (*19*). The fluctuations consisted of two periods of rapid regression followed by even more rapid transgressions over a total time interval of no more than a few million years (*19*). These changes in sea level, together with an associated climatic change, are thought to be responsible for the P-Tr extinction event (*19*).

If there is a connection between flood volcanism and mass extinction, the latter probably resulted from the injection of large amounts of SO_2 and volcanic dust into the atmosphere during volcanism. Sulfate aerosols in particular are known to produce acid rain and to have a global cooling influence (*20*). Five features of Siberian Trap volcanism make it likely that this event was more effective in producing global climatic change than other periods of flood volcanism. First, the Siberian Traps represent the largest subaerial volcanic event in the Phanerozoic record. Second, the comagmatic association of the Siberian Traps with mafic intrusions that host some of the world's richest magmatic, Cu-Ni-sulfide ore deposits indicates that many of the trap magmas carried a large amount of sulfur and that at least some were saturated with sulfur. Third, the trap magmas ascended through 5 to 5.5 km of sediments that contain abundant anhydrite, so they had the opportunity to entrain and exsolve sulfur from the upper crust as well as from the mantle. Fourth, the Siberian Trap sequence differs from that of most other flood basalt provinces in that it contains a significant pyroclastic component; approximately 20% by volume of the volcanic sequence is composed of tuffs. The effective degassing of sulfur requires the magma to vesiculate so that the gases are released before they become quenched into eruptive products (*21*). Finally, lithic fragments from the underlying sediments are abundant in the tuffs. Most of these fragments come from the Permian coal-bearing Tungussky suite, but some dolomites and marls are from the Devonian sequence 300 to 1500 m below the traps. Some rare fragments in tuff breccias originate from depths as great as 10 km. The widespread occurrence of lithic fragments in the tuffs testifies to the violent nature of the eruptions. In addition, because the Devonian and Carboniferous sequences contain abundant anhydrite, the eruptions almost certainly blasted large amounts of sulfate directly into the atmosphere. The P-Tr mass extinction may have resulted from a combination of acid rain and global cooling produced by sulfate aerosols.

A global cooling event, associated with the eruption of the Siberian Traps, also may have caused the sea-level fluctuations and P-Tr boundary. Changes in sea level reflect either shifts in the shape of the ocean basins brought about by global tectonics or changes in the amount of water available to the oceans. No tectonic process has been suggested that can produce a rapid, global marine regression-transgression event of the magnitude seen at the P-Tr boundary. Furthermore, the return of sea level to its approximate former position after the regression would require either that the tectonic process that caused the recession was reversed over no more than 1 or 2 million years or that it was followed by a second tectonic process that was approximately equal and opposite to the first. Both of these scenarios are improbable.

The global cooling produced by volcanic dust and sulfate aerosols may have been of sufficient intensity to produce a marked expansion in the global ice cap. This hypothesis explains the rapid onset of the regression and its short duration. Once volcanic emissions cease, the dust and SO_2 are rapidly purged from the atmosphere, the ice cap melts, and sea level returns to its approximate previous position.

Evidence of a brief ice age at the P-Tr boundary may be difficult to find in the geological record, especially because such a period would be associated with a marine regression. Well-exposed sedimentary sections across the P-Tr boundary are rare and only two known samples can be regarded as essentially complete (*22*).

REFERENCES AND NOTES

1. R. W. Griffiths and I. H. Campbell, *Earth Planet. Sci. Lett.* **99**, 66 (1990).
2. I. H. Campbell and R. W. Griffiths, *ibid.*, p. 79; P. R. Hooper, in *Continental Flood Basalts*, J. P. Macdougall, Ed. (Kluwer Academic, Dordrecht, the Netherlands, 1988), pp. 1–33; Y. Gallet, R. Week, D. Vandamme, V. Courtillot, *Earth Planet. Sci. Lett.* **93**, 273 (1989); P. R. Renne *et al.*, *Science* **258**, 975 (1992); R. White and D. McKenzie, *J. Geophys. Res.* **94**, 7685 (1989).
3. M. A. Richards, R. A. Duncan, V. E. Courtillot, *Science* **246**, 103 (1989).
4. M. R. Rampino and R. B. Stothers, *ibid.* **241**, 663 (1988).

5. J. C. Claoué-Long, Z. Zichao, M. Guogan, D. Shaohua, *Earth Planet. Sci. Lett.* **105**, 182 (1991).
6. P. R. Renne and A. R. Basu, *Science* **253**, 176 (1991).
7. G. B. Dalrymple *et al.*, *Eos* **72**, 570 (1991).
8. A. Baksi and E. Farrar, *ibid.*, p. 570.
9. G. A. Izett, G. B. Dalrymple, L. W. Snee, *Science* **252**, 1539 (1991).
10. J. L. Wooden *et al.*, *Eos* **72**, 571 (1991).
11. V. A. Fedorenko, *Sov. Geol. Geophys.* **22**, 66 (1981).
12. J. C. Claoué-Long, W. Compston, M. Fanning, J. Roberts, *Chem. Geol.*, in press.
13. The assumption of concordance can be tested by comparison of the mean to the mode and by recalculation of the mean after omission of all high-U grains. The mean is not significantly different from the mode, nor is it changed if high-U grains are omitted, which justifies the assumption of concordance.
14. L. P. Zonenshain, M. I. Kuzmin, L. M. Natapov, Eds., *Geology of the USSR: A Plate-tectonic Synthesis*, vol. 21 of *Geodynamics Series* (American Geophysical Union, Washington, DC, 1990); G. F. Makarenko, *Int. Geol. Rev.* **19**, 1089 (1977).
15. A. N. Khramav and V. P. Rodionov, in *Global Reconstructions and the Geomagnetic Field During Palaeozoic*, M. W. McElhinny, Ed. (Kluwer Academic, Dordrecht, the Netherlands, 1981), vol. 10, pp. 99–115; E. Irving and L. G. Parry, *Geophys. J. R. Astron. Soc.* **7**, 395 (1963); J. G. Ogg and M. B. Steiner, *Earth Planet. Sci. Lett.* **107**, 69 (1991).
16. M. Haag and F. Heller, *Earth Planet. Sci. Lett.* **107**, 42 (1991).
17. V. V. Zolotukhin and A. I. Al'Mukhamedov, in *Continental Flood Basalts*, J. D. Macdougall, Ed. (Kluwer Academic, Dordrecht, the Netherlands, 1988), pp. 273–310.
18. D. M. Raup and J. J. Sepkoski, Jr., *Science* **231**, 833 (1986).
19. W. T. Holser and M. Magaritz, *Mod. Geol.* **11**, 155 (1987); W. T. Holser *et al.*, *Nature* **337**, 39 (1989).
20. J. B. Pollack, O. B. Toon, E. F. Danielsen, D. J. Hofman, J. M. Rosen, *Geophys. Res. Lett.* **10**, 989 (1983); D. J. Hofmann and J. M. Rosen, *J. Geophys. Res.* **92**, 9825 (1987); M. R. Rampino and S. Self, *Nature* **310**, 677 (1984); S. Self and M. R. Rampino, *Eos* **69**, 83 (1988).
21. H. Sigurdsson, in "Global Catastrophes in Earth History: An Interdisciplinary Conference on Impacts, Volcanism, and Mass Mortality," V. L. Sharpton and P. D. Ward, Eds. *Geol., Soc. Am. Spec. Pap. 247* (1990), pp. 99–110.
22. W. T. Holser and M. Margaritz, *Geochim. Cosmochim. Acta* **66**, 3297 (1992).

23. We thank D. Devir and J. Bitmead for their assistance in preparing the manuscript.

1 May 1992; accepted 23 September 1992

Manipulation of the Reconstruction of the Au(111) Surface with the STM

Y. Hasegawa and Ph. Avouris*

Modification of the reconstruction of an Au(111) surface with a scanning tunneling microscope (STM) is demonstrated. This modification is accomplished by transferring a number of surface atoms to the STM tip to generate a surface multivacancy (hole), which modifies the stress distribution at the surface. The structural changes that follow the tip-induced surface perturbation are imaged in a time-resolved manner. The structural modification is the result of both short-range interactions, which lead to local atomic relaxation, and long-range elastic interactions, which produce large-scale rearrangements.

In recent years, the STM (*1*) has emerged as a unique tool for the atomic and nanometer-scale modification and manipulation of materials (*2*, *3*). In particular, experimental approaches have been developed that allow the reversible transfer of atoms between the sample and the STM tip by means of chemical tip-sample interactions and voltage pulses (*4*, *5*). Here, we demonstrate the manipulation of the reconstruction of the Au(111) surface. This reconstruction involves an array of surface dislocations whose pattern we are able to modify with the STM. To accomplish this, we induce "local" perturbations by transferring a number of surface atoms to the tip (*4*). The resulting vacancy modifies the stress distribution at the surface, and through substrate-mediated long-range elastic interactions it leads to large-scale atomic rearrangements. We are able to follow these atomic relaxation processes in a time-resolved manner, and we find evidence not only of single atom motion (diffusion) but also of concerted motion of large numbers of atoms. An important implication of this work is that, because of the elastic coupling between surface atoms, there are limits, which are material-dependent, to how small and how local STM-induced modifications can be.

A variety of diffraction techniques (*6*–*8*) and the STM (*9*–*11*) have been used to study the reconstruction of the Au(111) surface, which has a $22 \times \sqrt{3}$ structure (that is, a structure with a unit cell whose sides are, respectively, 22 and $\sqrt{3}$ times the nearest neighbor Au atom distance in the unreconstructed surface). This surface structure is considered to be the result of a balance between two opposing tendencies (*12*): the surface layer would like to contract in order to compensate for its reduced coordination, whereas opposing this contraction the underlying substrate potential favors a commensurate surface layer. The misfit between the surface layer and the substrate leads to the formation of a periodic array of pairs of partial dislocations (domain walls), which separate alternating domains in which surface atoms occupy face-centered-cubic (fcc) and hexagonal close-packed (hcp) sites (Fig. 1). The surface atoms at the dislocation lines occupy bridge instead of hollow sites, and in STM images of the surface (Figs. 2 and 3) the dislocation lines appear as ridges with a height of ~0.1 to 0.2 Å. The unit cell of this reconstruction (22 times the unit length) contains 23 surface atoms instead of 22, thus allowing a 4.4% contraction along the $\langle 1\bar{1}0 \rangle$ direction in the surface layer. Because of the small energy difference between fcc and hcp sites, the widths of fcc and hcp domains are different; the wider domain is presumed to have the fcc structure, which is energetically more favored. Although the $22 \times \sqrt{3}$ reconstruction relieves the stress along the $\langle 1\bar{1}0 \rangle$ direction, stress remains in other directions.

To relieve the stress in a more uniform manner, a surface superstructure is formed consisting of a regular alternation of uniaxial domains arranged in a zigzag pattern. This rotational domain superstructure, usually referred to as a herringbone structure, is energetically favored because of the substrate-mediated elastic interactions between the rotational domain boundaries (*13*, *14*). Because the reduction of surface stress is the main driving force for this reconstruction, the surface structure is expected to be sensitive to perturbations that affect the stress distribution at the surface.

From a study of large numbers of STM images, we find that there is a strong tendency for the dislocation lines to be perpendicular to the surface steps. Steps are free edges of the surface layer, and therefore the stress component perpendicular to the steps must be zero. Because surface stress is still present along the dislocation lines, these lines tend to align themselves perpendicular to the steps so as to relieve the surface stress. This observation suggested that, if step-like structures can be made artificially on the surface, the pattern of dislocation lines could be modified intentionally and the structural changes that take place could be imaged with the STM. For example, an STM-generated hole (multivacancy) on the surface is surrounded by steps and thus should be able to relieve the surface stress around it.

In this work, we applied voltage pulses between the STM tip and the sample to remove surface atoms, generate holes at specific surface locations, and thus modify the surface reconstruction (pattern of dis-

IBM Research Division, T. J. Watson Research Center, Yorktown Heights, NY 10598.

*To whom correspondence should be addressed.